



Missouri University of Science and Technology
Scholars' Mine

International Conferences on Recent Advances in Geotechnical Earthquake Engineering and Soil Dynamics 2010 - Fifth International Conference on Recent Advances in Geotechnical Earthquake Engineering and Soil Dynamics

29 May 2010, 8:00 am - 9:30 am

Experimental Study of the Dynamic Interaction Between the Foundation of the NEES/UCSD Shake Table and the Surrounding Soil

Ozgur Ozelik
Dokuz Eylul University, Turkey

J. Enrique Luco
University of California San Diego, La Jolla, CA

Joel P. Conte
University of California San Diego, La Jolla, CA

Luis H. Mendoza
CICESE, Mexico

Follow this and additional works at: <https://scholarsmine.mst.edu/icrageesd>

 Part of the [Geotechnical Engineering Commons](#)

Recommended Citation

Ozelik, Ozgur; Luco, J. Enrique; Conte, Joel P.; and Mendoza, Luis H., "Experimental Study of the Dynamic Interaction Between the Foundation of the NEES/UCSD Shake Table and the Surrounding Soil" (2010). *International Conferences on Recent Advances in Geotechnical Earthquake Engineering and Soil Dynamics*. 6.

<https://scholarsmine.mst.edu/icrageesd/05icrageesd/session08/6>

This Article - Conference proceedings is brought to you for free and open access by Scholars' Mine. It has been accepted for inclusion in International Conferences on Recent Advances in Geotechnical Earthquake Engineering and Soil Dynamics by an authorized administrator of Scholars' Mine. This work is protected by U. S. Copyright Law. Unauthorized use including reproduction for redistribution requires the permission of the copyright holder. For more information, please contact scholarsmine@mst.edu.



Fifth International Conference on

Recent Advances in Geotechnical Earthquake Engineering and Soil Dynamics and Symposium in Honor of Professor I.M. Idriss

May 24-29, 2010 • San Diego, California

EXPERIMENTAL STUDY OF THE DYNAMIC INTERACTION BETWEEN THE FOUNDATION OF THE NEES/UCSD SHAKE TABLE AND THE SURROUNDING SOIL

Ozgur Ozelik

Dokuz Eylul University
Izmir, Turkey 35160

J. Enrique Luco

University of California, San Diego
La Jolla, CA 92093

Joel P. Conte

University of California, San Diego
La Jolla, CA 92093

Luis H. Mendoza

CICESE, Ensenada
Baja California, Mexico

ABSTRACT

The results of an extensive experimental study of the dynamic interaction between the foundation block for the NEES/UCSD Large High Performance Outdoor Shake Table and the surrounding soil are presented. The vibrations induced by the two large NEES/UCLA eccentric mass shakers were recorded at multiple stations within the reinforced concrete foundation block and on the soil up to distances of 270 m from the block. The results obtained for the deformation pattern of the reaction block, the frequency response at selected stations on the block, and the average rigid-body motion of the foundation and its dependence on frequency for longitudinal (EW) excitation are presented in detail. Comparison of the response during shaker-induced vibrations with that resulting from the much stronger actuator forces shows that linearity holds for the range of forces involved. The attenuation of the ground motion away from the reaction block is also described.

INTRODUCTION

The construction of the foundation block for the NEES/UCSD Large High Performance Outdoor Shake Table (Fig. 1) which is part of the George E. Brown, Jr. Network for Earthquake Engineering Simulation (NEES) created a rare opportunity for an extensive experimental study of dynamic soil-foundation interaction effects. The large forces that the actuators of the shake table exert on the reaction block and the soil suggested the need to determine the induced ground motion in the vicinity of the table, as well as the need to evaluate the effects that any motion of the block itself would have on the control of the shake table. Although the shake table would operate initially with only longitudinal motion, it was designed to be upgradeable to six degrees of freedom. For this reason, it was necessary to estimate the response of the foundation block to at least longitudinal, transverse and torsional excitation. To simulate the forces that the actuators would exert on the reaction block, the two large NEES/UCLA MK-15 eccentric mass shakers with a maximum force capacity of 0.445 MN (100,000 lbs) each were mounted on the block at locations near the intended supports of the actuators. In tests conducted in October 21-24, 2003, the three-dimensional dynamic response at 19 locations on the reaction block; at 12 points on the foundation of the adjacent auxiliary building; and at 33 locations on the ground surrounding the shake table up to

distances of over 270 m were recorded for longitudinal, transverse, and torsional excitation of the block. The frequency range of 0 to 20 Hz selected for the tests reflected the frequency range of operation of the table (0-33 Hz), the frequency limitations of the shakers (25 Hz), and the maximum force capacity of the shakers.

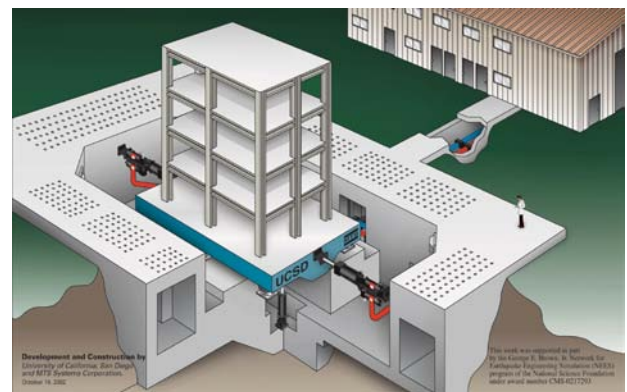


Fig. 1. Schematic representation of NEES/UCSD Shake Table.

The first objective of the experimental study was to obtain dynamic ground motion data, and by inference geotechnical data, that will prove invaluable in the development of a future virtual model of the complete NEES/UCSD Shake Table Facility including a soil island surrounding the shake table and adjacent soil pit, and models for the reinforced concrete foundation block, the steel platen, actuators and control system, and of the test specimens (Ozcelik, 2006). The second objective of the study was to develop a body of dynamic high-quality response data on the foundation and surrounding soil that can be used to test and validate soil-structure interaction analysis methods and computer codes. In particular, the data would offer experimental information on the coupling through the soil between adjacent foundations. The final objective was to validate the unconventional design of the NEES/UCSD foundation block in terms of its overall dynamic response, and to study experimentally the deformability of the foundation and surrounding soils. The design of the NEES/UCSD foundation took advantage of the natural conditions at the site in terms of high soil stiffness to build a lighter and considerably less costly foundation which resulted in a high characteristic frequency and a large effective damping ratio as opposed to the conventional design which relies on the use of massive foundations to achieve a low characteristic frequency.

CHARACTERISTICS OF THE FOUNDATION BLOCK AND SURROUNDING SOIL

Description of the Foundation Block

The reinforced concrete foundation block for the shake table is 19.61 m (64.33 ft) wide, 33.12 m (108.67 ft) long, and extends to a depth of 5.79 m (19 ft). A smaller central area of the foundation housing the hold down struts extends to a depth of 7.92 m (26 ft). To reduce the mass of concrete, the corners of the block have been truncated and the structure has been designed as a hollow tube along the perimeter (Figs. 2 and 3). The mass of the reaction block is 4.4×10^6 kg. A 6.10 m (20 ft) long tunnel with a 2.44m x 2.44 m (8 ft x 8 ft) section connects the reaction block to the adjacent pump building, which is a 2-storey structure with a partial basement. The pump building has plan dimensions of 15.5 m x 22.5 m and is founded at a depth of 3.5 m. A soil pit to the east of the shake table has dimensions of 14.6 m x 15.2 m and a maximum depth of about 5.8 m.

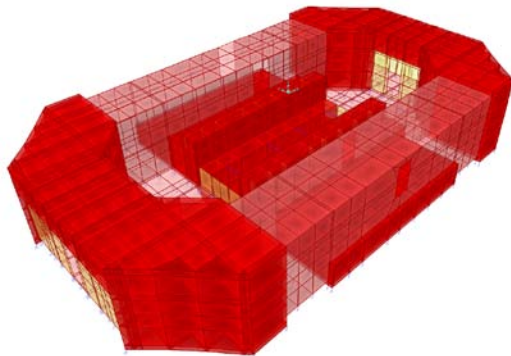


Fig. 2. 3D rendering of reaction block.

The reaction block supports the moving steel platen of the NEES Shake Table which is 7.62 m (25 ft) wide, 12.19 m (40 ft) long, and has an effective mass of 144,000 kg. In the initial phase of the facility, the motion of the table is uni-directional with a maximum stroke of 0.75 m, a peak horizontal velocity of 1.8 m/s, a peak horizontal acceleration of 4.2 g for bare table conditions and 1.2 g under a payload of 400 tons, an overturning moment capacity of 50 MN-m, and a vertical payload capacity of 20 MN. The testing frequency range of the table is 0-33 Hz. In the initial phase the system has two servo-controlled dynamic actuators with a combined total horizontal force capacity of 6.8 MN. The facility has an innovative vertical load/ overturning moment bearing system including six pressure balance bearings and two hold down struts (Van den Einde, 2004; Conte et al, 2004; Ozcelik et al, 2008a, 2008b)). The forced vibration tests described here were conducted on the bare reinforced concrete reaction block (Fig. 3) before the platen, bearings and actuators were installed.



Fig. 3. NEES/UCLA MK-15 Shaker attached at the East end of the reaction block.

Geological and Geotechnical Characteristics of the Site

The site for the LHPOST occupies approximately 1.2 acres of land at the northwest end of the UCSD Englekirk Earthquake Engineering Research Center located in the Scripps Ranch area of San Diego, California. A field investigation (Geocon, 2002) including four exploratory borings drilled to depths varying from 1.8 to 21.6 m (6 to 71 ft) indicates that three general soil types underlie the site. Topsoils with a thickness varying from 0.6 to 0.9 m (2 - 3 ft) cover the site. These soils are characterized as firm, sandy clay with gravel and cobble and loose clayey sand with gravel and cobble. Quaternary soils of the LindaVista Formation underlie the topsoils and extend to approximately 3.7 m (12 ft) below the existing elevation. The soils of this formation are characterized as very dense, clayey sands with gravel and cobble. Tertiary soils of the Stadium Conglomerate were found beneath the soils of the LindaVista Formation. These soils are characterized as very dense silty sand to sandy, cobbly gravel.

Laboratory tests of undisturbed samples obtained from a boring that extended to a depth of 18.3 m (60 ft) resulted in an average in-place dry unit weight of 157 N/m³ (107.2 pcf) and an average moisture content of 10.25% for the Stadium Conglomerate. The corresponding values for the topsoils were 168 N/m³ (114.6 pcf) and 8.65%, respectively. Results of a direct shear test on a sample taken at a depth of 4.25 m (14 ft) show a unit cohesion of 47.9 Pa (200 psf) and an angle of shear resistance of 38 degrees (Geocon, 2002). The logs of borings separated by about 46 m (150 ft) show significant lateral differences within the Stadium Conglomerate at depth below 3.7m (12 ft) from the surface.

Measurements of the shear-wave velocities at the site resulted in values of 185 to 305 m/sec (600 to 1,000 ft/sec) for the LindaVista Formation and 760 m/sec (2,500 ft/sec) for the Stadium Conglomerate (S. Ashford, personal communication).

FORCED VIBRATION TESTS

The forced vibration tests on the reaction block of the NEES@UCSD Shake Table were conducted using the equipment and personnel from the NEES@UCLA Earthquake Engineering Field Laboratory (Stewart et al, 2005) supplemented with equipment and personnel from the Centro de Investigacion Cientifica y de Educacion Superior de Ensenada (CICESE), Mexico. The NEES@UCLA equipment included two MK-15 Shakers, 55 EpiSensor accelerometers, 17 Quanterra Q330 data loggers, and a mobile command center.

Characteristics of the MK-15 Shakers

The two large NEES/UCLA MK-15 shakers (ANCO Engineering, Boulder, Colorado) are uni-directional shakers with counter-rotating weights with an operating frequency range of 0-25Hz, and a peak force of 445 KN (100,000 lbs) each. Each of the two MK-15 shakers is fitted with two basket assemblies that counter rotate in a horizontal plane. Each basket assembly consists of four segments (baskets # 1, 2, 3, 4) and a counterweight. The baskets have been designed to accept 5cm × 10cm × 20cm (5in × 10in × 20in) steel bricks as a means of adjusting the total eccentricity (WR) of the system from 15.6 N-m (138lb-in, empty baskets with counterweight) to 11,220 N-m (99,295lb-in, baskets 1-4 filled with a total of 82 bricks) per basket assembly. Each shaker is driven by a 50HP motor, which is equipped with a Vector drive (controller), which allows setting frequency to 0.1% FS accuracy over the 1%-100% speed range. The controller also allows programming a step-sweep over a given frequency range and has a wireless control option. The system has a front panel digital display of frequency and a 1-pulse/revolution phase signal. In addition, a dual synchronized drive allows the two MK-15 shakers to run in phase lock (in-phase or out-of-phase). Within each shaker, the

two rotating arms are synchronized mechanically.

Each MK-15 shaker with two counter-rotating eccentric weights produces a uni-directional sinusoidal force (F) which increases in direct proportion to the eccentricity (WR) and to the square of the rotating frequency (f [Hz]) as

$$F(t) = 2 \times (WR / g) \times (2\pi f)^2 \times \sin(2\pi ft) \quad (1)$$

The amplitude of the force per shaker (in lbs) can be written as

$$F = 0.205 \times WR \times f^2 \quad (2)$$

where the eccentricity WR is expressed in lb-inches.

In the tests described here, only the small basket was used with one or four bricks (laying flat) per basket. The corresponding eccentricities WR are 761.4 and 1,185.4 lb-in, respectively (R. S. Keowen, personal communication). The resulting amplitudes of the force per shaker at 10 Hz are F=15,609 lb (0.0694 MN) for one brick and F=24,301 lb (0.108 MN) for 4 bricks. As shown in Fig. 3 the MK-15 shakers were attached to the East and West ends of the reaction block immediately above the reaction areas of the longitudinal actuators.

Sensors and Data Acquisition System

The instrumentation used in the experiments included 10 Triaxial EpiSensor Force Balance Accelerometers (NEES@UCLA), 45 Uniaxial EpiSensor Force Balance Accelerometers (NEES@UCLA), and 30 Uniaxial Mark Velocity Sensors (CICESE). The Kinometrics EpiSensor accelerometers have a dynamic range of 140dB (uniaxial) and 155dB (triaxial), a bandwidth of DC to 200Hz, a full-scale range of +/- 2g, and an output of +/- 20V differential. The Mark L-4C 1.0Hz geophone with a coil resistance of 5500 Ohms has a transduction constant of 7.02 V/(in/sec).

The uniaxial EpiSensor accelerometers were first bolted in triaxial packages to 20cm × 20cm × 0.64cm (8in × 8in × 1/4in) aluminum plates which were secured to the ground by four 10cm (4-inch) long corner spikes or bolted to the concrete of the foundations. The triaxial accelerometers were also attached to similar plates. The Mark seismometers were secured in place by sand bags.

The total number of acceleration and velocity channels recorded simultaneously amounted to 105 channels. In addition, 4 pulser channels (2 per MK-15 shaker) were used to record the location of the rotating baskets and to provide information to determine the phase of the harmonic shaker force. The 109 channels of data were acquired using 17 6-channel (NEES@UCLA) and 3 3-channel (2 UCSD, 1 IRIS) Quanterra Q330 data acquisition systems. The Kinometrics Quanterra Q330 data loggers include a 24-bit A/D converter, a GPS receiver for time stamping for synchronization across

multiple nodes, a local memory buffer and a communication module. The system used had a sampling rate of 200 samples per second, a gain of one, an input range of 40 V peak-to-peak, a 135dB dynamic range, and a time stamp (time synchronization) accuracy of < 0.1ms.

In the NEES@UCLA field data acquisition system (Stewart et al, 2005), the accelerometers (grouped in clusters of 6 channels each) transmit analog signals to the 6-channel Q330 data loggers in which they are digitized, time-stamped and stored in a local memory buffer as data packets. From there, the data packets are sent to the data concentration point using Transmission Control Protocol/Internet Protocol (TCP/IP) via IEEE 802.11b long-range wireless radios. The data concentration point contains a Sun Microsystems Netra 120 server running Antelope data acquisition software (Boulder Real Time Technologies 2006) to centrally record data packets received from each of the various Quanterra Q330 nodes. Finally, the Antelope server in the data concentration point transmits wirelessly, using an orb2orb transfer protocol, all of the received data packets to a laptop computer inside the mobile command center also running Antelope software. The laptop computer was used to observe the experiment in real-time using the Antelope real-time monitoring (Antelope RTM) system

Instrumentation of the Reaction Block and Adjacent Foundations

The reaction block was instrumented with 10 triaxial EpiSensor accelerometers (or packages of three uniaxial accelerometers) placed on the top surface of the block (RT1-RT10), 8 triaxial accelerometers (RB1-RB8) placed at the base of the block (5.18 m from the top), and one triaxial accelerometer (RB9) located at a sump at the center of the base of the block (6.2 m from top of block). The locations of the stations are shown in Fig. 4(a).

The foundation of the pump building was instrumented with 6 triaxial arrangements of EpiSensor accelerometers (P1-P6). The tunnel connecting the reaction block and the pump building was instrumented with 2 triaxial arrangements of Mark seismometers (T1-T2). Finally, the foundation of the Blast Simulator was instrumented with 4 triaxial arrangements of Mark seismometers (B1-B4). For reference, the three-dimensional motion of the soil at four stations (SSW, SSE, SNE, and SNW) adjacent to the reaction block was recorded with triaxial arrangements of Mark seismometers. The combined array of sensors included 31 tri-axial stations on the foundations and four tri-axial stations on the soil adjacent to the reaction block.

Instrumentation of the Free-Field Ground Surface

Four linear arrays extending to the east, west, north and south of the reaction block were used to instrument the free-field

ground surface (Fig. 4b). The geometry of the arrays was selected by consideration of the number of sensors available, of the boundaries of the Camp Elliot site, and the presence of natural or man-made obstacles. The longest array extended 244 m to the south and included nine stations (S0-S8) placed at progressively larger distances from the edge of the reaction block (0, 7.6, 18.3, 52, 170, 120, 380, 169 and 244 m).

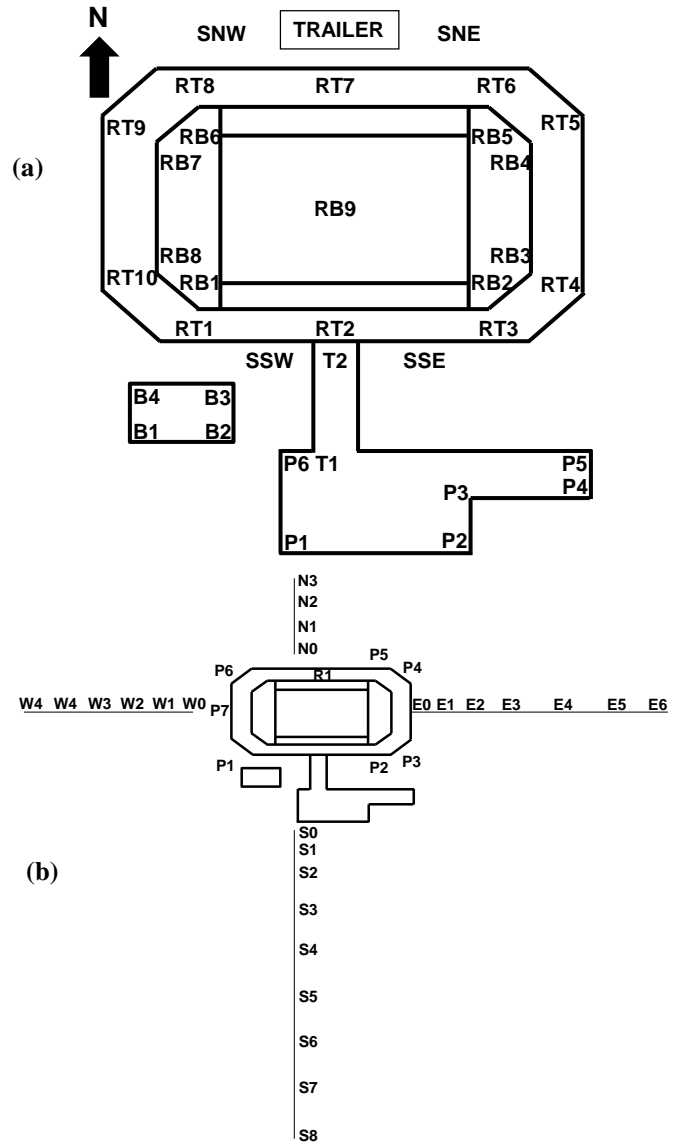


Fig. 4. Instrument locations on (a) Reaction Block and adjacent foundations, and (b) surrounding soil.

All nine stations were instrumented with Mark seismometers in triaxial arrangements. All other arrays were instrumented with triaxial EpiSensor accelerometers or with uniaxial accelerometers in triaxial arrangements. The array to the east included 7 stations (E0-E6) located at distances of 0, 19.8, 45.7, 83.8, and 98.8 m from the reaction block. The array to the north included four stations (N0-N3) placed at distances of 0, 7.6, 18.3, and 29.3 m from the edge of the reaction block. Finally, the array to the west included six stations (W0-W5)

located at distances of 0, 7.6, 18.3, 33.8, 53, and 76.5 m from the edge of the foundation. In addition, 7 stations (P1-P7) were placed on the soil along the perimeter of the reaction block.

In total, 99 components of three-dimensional ground motion were recorded at 33 locations on the soil adjacent to the reaction block. A reference station (RT7) with a triaxial EpiSensor was kept on the reaction block during all of these tests.

Sequence of Tests

The number of sensors and data acquisition channels available for the experiment was of the order of 110 channels. This limitation made it necessary to conduct two sets of tests to satisfy the need to obtain the dynamic response of the foundation block and of surrounding soil at a large number of locations. In the first set of 8 tests (Tests 1-8), most sensors were placed on the reaction block and on the foundations of the adjacent pump building and blast simulator. In the second set of 9 tests (Tests 9-17), most sensors were placed on linear arrays extending from the reaction block into the surrounding soil. In this paper we consider only tests involving longitudinal (EW) excitation of the block (Tests 1, 2, 14, 17). The tests included excitation with one (Test 1) and two shakers acting in phase (Tests 2, 14, 17). To check for linearity, Tests 14 (4 bricks per basket) and 17 (1 brick per basket) were conducted at two different levels of force. The forced vibration tests covered frequencies ranging from 1 to 18 Hz or 5 to 20 Hz depending on the level of force (Table 1).

Table 1. Vibration Tests involving EW Excitation

Test No	Area Instrumented	Shaker(s)	Phase	Force Level	Freq. Range
1	Foundations	E		4 Bricks	1-18 Hz
2	Foundations	E+W	0	4 Bricks	1-18 Hz
14	Soil	E+W	0	4 Bricks	1-18 Hz
17	Soil	E+W	0	1 Brick	5-20 Hz

RESPONSE OF THE REACTION BLOCK TO LONGITUDINAL (EW) EXCITATION

At the present time, the NEES/UCSD shake table operates one-directionally in the longitudinal (EW) direction. For this reason it is important to consider first the response of the block to EW excitation with the two shakers acting in phase. In the case of Test 2 with four bricks in each basket, the combined harmonic total force exerted by the shakers at a frequency of 10 Hz has an amplitude of 0.216MN (48,602 lb). The corresponding three-dimensional accelerations recorded at the top and base of the reaction block for an excitation

frequency of 10 Hz are shown in Figs. 5 and 6, respectively. Fig. 5 shows a sample of the time histories of the x-East (column a), y-North (column b) and z-vertical (column c) components of acceleration for the 10 stations (RT1-RT10) at the top of the reaction block. Each frame in Fig. 5 includes the traces of the accelerations at two stations symmetric with respect to the EW axis. Referring to the x-EW component (column a) it is apparent that: (i) the motion is symmetric with respect to the EW axis of the block, (ii) the central core (RT1, RT2, RT3, RT6, RT7, RT8) translates almost as a rigid body, (iii) the accelerations at both ends of the block near the shakers (RT4 and RT5, RT9 and RT10) are larger than in the central core indicating out-of-plane deformation of the East and West walls, and (iv) the largest accelerations of about 0.39% g occur at the East end of the block adjacent to the (then) empty soil pit. Column (c) in Fig. 5 shows the vertical accelerations recorded on top of the block. The results indicate that: (i) the vertical accelerations are symmetric with respect to the EW axis but anti-symmetric with respect to the NS axis of the block, (ii) the amplitudes of the vertical accelerations increase with distance to the NS axis indicating rocking of the reaction block about a NS axis, and (iii) the largest vertical accelerations of about 0.26% g occur at the East end of the block adjacent to the empty soil pit.

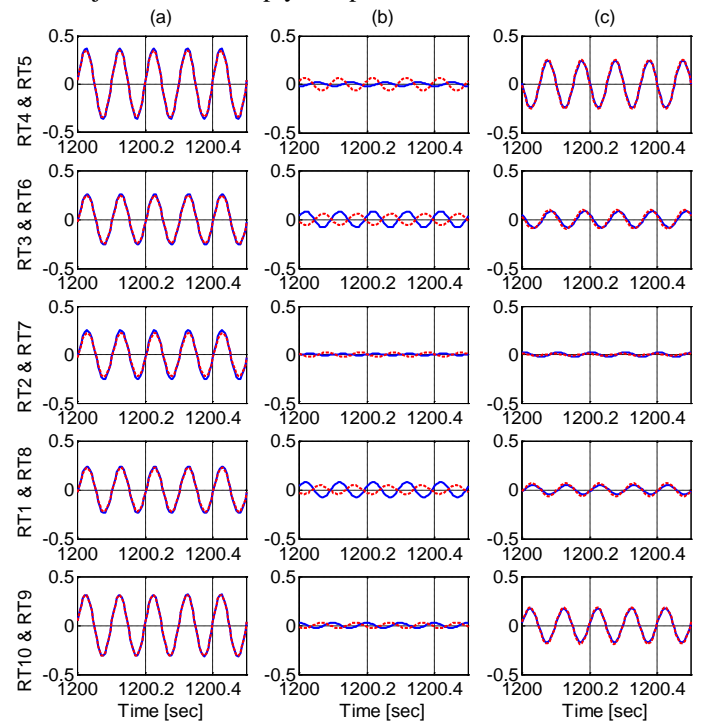


Fig. 5. Sample of time-histories of the (a) East, (b) North, and (c) Vertical acceleration components (%g) at the top of the reaction block (stations RT1-RT10) for EW excitation at 10 Hz (Test 2).

Finally, the results for the y-North components of acceleration shown in column (b) indicate that: (i) the NS motion is mostly anti-symmetric with respect to the EW axis of the block, (ii) the NS motion at station RT2 located next to the tunnel is small suggesting a restraining effect by the tunnel, and (iii) the NS accelerations with a maximum amplitude of about 0.08% g

are significantly smaller than the EW and vertical components.

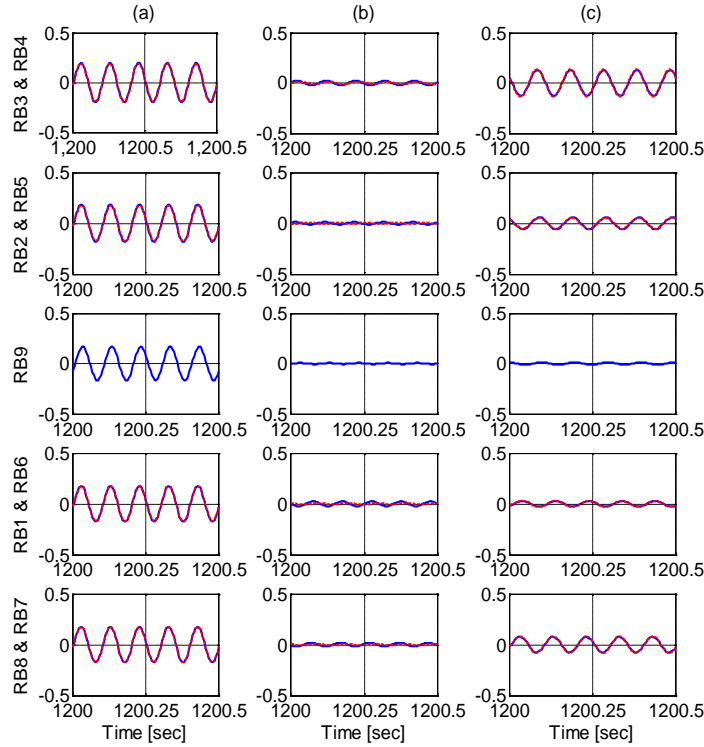


Fig. 6. Sample of time-histories of the (a) East, (b) North and (c) Vertical acceleration components (%g) within the reaction block (stations RB1-RB9) for EW excitation at 10 Hz (Test 2).

Samples of the time-histories of the x-East (column a), y-North (column b) and z-vertical (column c) components of acceleration for the 9 stations (RB1-RB9) within the reaction block are shown in Fig. 6. Again, each frame in Fig. 6 includes the traces of the accelerations at two stations symmetric with respect to the EW axis. The response within the block shown in Fig. 6 is qualitatively similar to the response at the top of the block, but it shows more uniformity suggesting less deformation at the lower levels of the block.

DEFORMATION PATTERN OF THE REACTION BLOCK

The displacement and deformation pattern of the reaction block for harmonic EW excitation with a frequency of 10 Hz is shown in Figs. 7a, b, c and d. Figure 7a shows the initial geometry of the perimeter of the reaction block at ground level and the exaggerated deformed configuration in which the horizontal displacements have been scaled up by a factor of 10^6 . Also shown are the 10 recording stations (full circles) and their corresponding deformed positions (full triangles). The deformed perimeter was obtained by fitting a 5-parameter polynomial in x, y and z to the observed displacements at all 19 stations.

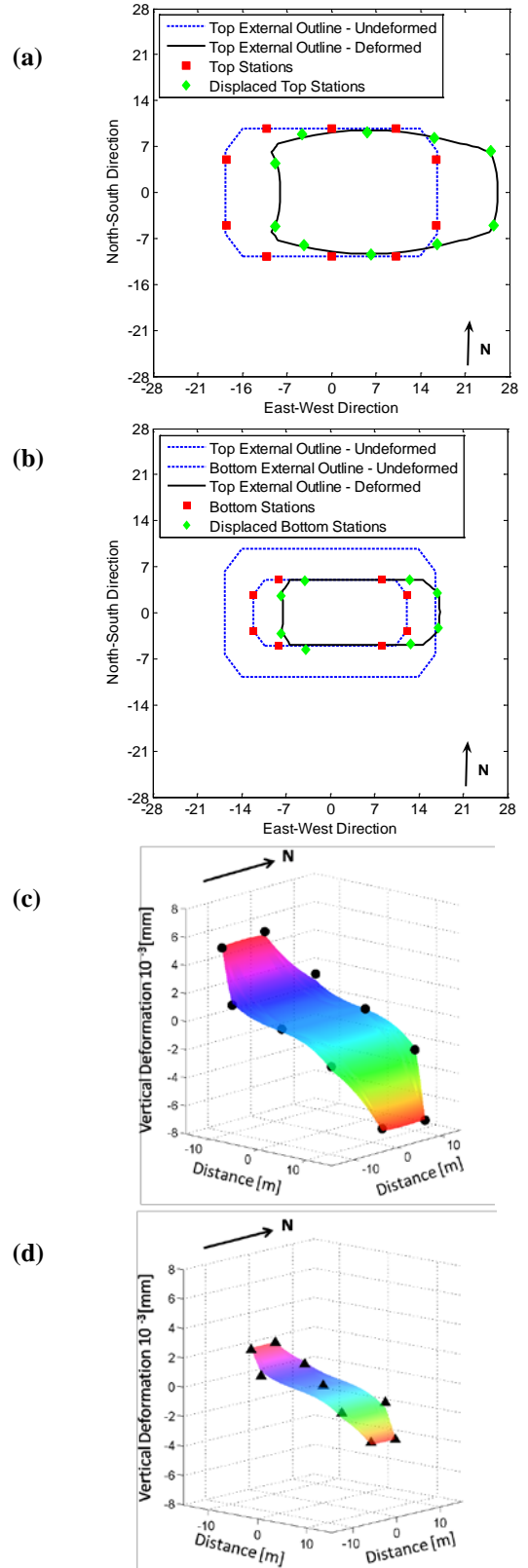


Fig. 7: Displacement and deformation of the reaction block for EW excitation at 10 Hz: Horizontal deformation at the top (a) and within (b) the block, and distribution of vertical displacements on horizontal plane at the (c) top and (d) bottom of the block.

The deformation of a lower level within the block is shown in Fig. 7b. The results in Figs. 7a and 7b show EW translation of the block, and out-of-plane bending of the East and West walls and, to a lesser degree, of the North and South walls. The EW displacements of the East wall are larger than those on the opposite wall. This difference is related to the unfilled soil pit to the east of the block.

Figures 7c and 7d show the amplitudes of the vertical displacements recorded at 19 stations plotted versus the (x, y) coordinates of the stations. Also shown in Figs. 7c and d is the vertical displacement pattern obtained by fitting a 5-parameter polynomial in x and y (but independent of z) to the recorded data at all 19 stations. The results in the figures confirm that the central portion of the block (RT1, RT3, RT6 and RT8) moves approximately as a rigid body, that there is bending of the East and West ends of the block, and that the vertical displacements recorded at the top of the block are consistent with those recorded within the block (i.e. that the walls are essentially rigid in the vertical direction).

FREQUENCY RESPONSE FOR EW EXCITATION

The amplitude of the EW and vertical frequency response of the block is illustrated in Figs. 8a and 8b, respectively. The displacement amplitudes have been scaled linearly to a harmonic force of constant amplitude 6.8 MN corresponding to the maximum force that the actuators can exert on the reaction block. The recorded accelerations were transformed to scaled displacements by multiplication by the factor $(6.8/0.216) \times (2\pi \times 10 / \omega)^2 / \omega^2$. The amplitudes shown in Fig. 8a correspond to the averages of the EW components

$$T3 = (RT4 + RT5 + RT9 + RT10)/4 \quad (3a)$$

$$T2 = (RT1 + RT3 + RT6 + RT8)/4 \quad (3b)$$

$$T1 = (RT2 + RT7)/2 \quad (3c)$$

$$B3 = (RB3 + RB4 + RB7 + RB8)/4 \quad (3d)$$

$$B2 = (RB1 + RB2 + RB5 + RB6)/4 \quad (3e)$$

$$B1 = RB9 \quad (3f)$$

The results in Fig. 8a indicate that: (i) the EW frequency response peaks at 10 Hz and has a peak amplification of the order of $2.6/2=1.3$, (ii) the average displacements T1 and T2 at the top of the block are very similar indicating that the central portion of the top of the block translates as a rigid body, (iii) the average displacement T3 at stations close to East and West ends of the block is about 50% larger than the displacements T1 and T2 indicating out-of-plane deformation of the East and West end walls, (iv) the average B3 is only slightly larger than the average B2 indicating only a small deformation of the East and West areas within the block, and (v) the EW motions increase with elevation indicating the presence of a rocking component.

The amplitudes shown in Fig. 8b correspond to the averages of the vertical components:

$$VT3 = (RT9 + RT10 - RT4 - RT5)/4 \quad (4a)$$

$$VT2 = (RT1 + RT8 - RT3 - RT6)/4 \quad (4b)$$

$$VB3 = (RB7 + RB8 - RB3 - RB4)/4 \quad (4c)$$

$$VB2 = (RB1 + RB6 - RB2 - RB5)/4 \quad (4d)$$

The results in Fig. 8b indicate that the amplitudes of the vertical displacements increase with horizontal distance to the NS axis of rotation at least for frequencies below 15 Hz. The distances to the NS axis from the stations at which the averages (VB2, VT2, VB3, VT3) are calculated correspond to (8.16, 10.20, 12.14, 16.46) m, respectively. The amplitude ratios VT3/VB2, VB3/VB2, and VT2/VB2 at 10 Hz are 5.00, 2.43, and 1.67, respectively, while the ratios of the corresponding distances are 2.02, 1.49, and 1.25. This comparison indicates that there is vertical deformation of the reaction block in addition to rocking about the NS axis as shown in Fig. 7b.

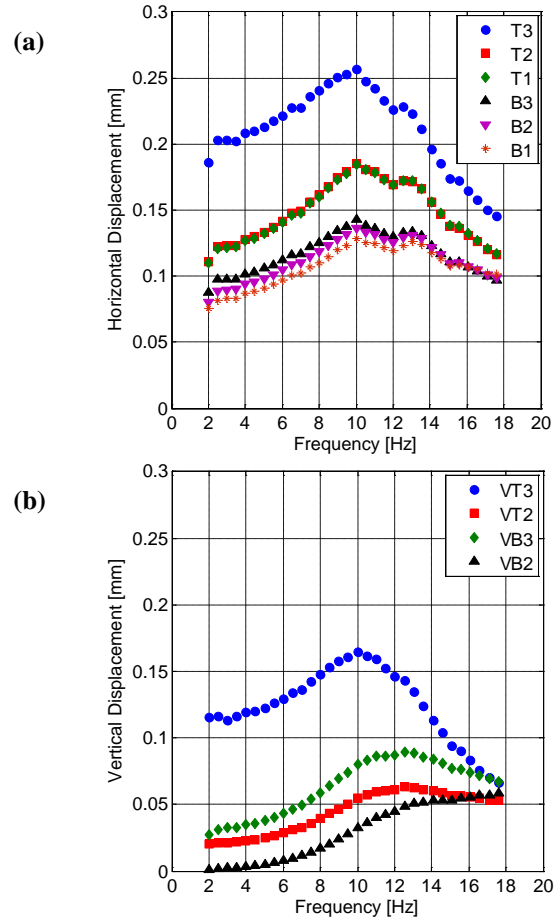


Fig. 8: Amplitudes of the (a) EW and (b) vertical frequency response of the reaction block for EW excitation. The results shown are based on Test 2 and correspond to scaled displacement amplitudes for a harmonic force of constant amplitude 6.8 MN.

The results in Figs. 8a and 8b for the average T3 of the motion at stations RT4, RT5, RT9 and RT10, indicate that the maximum scaled horizontal and vertical displacements for the maximum theoretical harmonic actuator force of 6.8 MN would be about 0.26 mm and 0.17 mm, respectively. These displacements are sufficiently small to have no effect on the control of the shake table which relies on the assumption that the measured relative displacement of the platen with respect to the reaction block represents the absolute displacement of the platen. The peak velocities on top of the reaction block of 1.63 cm/sec (0.64 in/sec) and 1.07 cm/sec (0.42 in/sec) are below the threshold of 2.54 cm/sec (1 in/sec) considered necessary to cause difficulties with mechanical equipment on the block. The maximum horizontal and vertical accelerations on top of the block would be 10.4% g and 6.9% g, respectively.

ESTIMATE OF THE AVERAGE RIGID-BODY MOTION

To facilitate comparisons with simple analytical models that assume that the block is rigid, we calculate next the average rigid-body motion of the reaction block. The average rigid-body motion is defined by the 6×1 vector

$$\{\Delta_o\} = (\Delta_x \ \Delta_y \ \Delta_z \ l\theta_x \ l\theta_y \ l\theta_z)^T \quad (5)$$

where $(\Delta_x \ \Delta_y \ \Delta_z)$ is the displacement of a point of reference taken to correspond to the top center of the block, and $(\theta_x \ \theta_y \ \theta_z)$ are the rotations with respect to the coordinate axes (x-East, y-North, z-up). The scaling factor $l = 16.56m$ was taken as the half-length of the reaction block. The vector $\{\Delta_o\}$ is calculated by a least-squares fit to the recorded displacements $\{u_i\} = (u_{xi} \ u_{yi} \ u_{zi})^T$ at $N = 15$ stations on the block. The motions recorded at stations RT4, RT5, RT9 and RT10 were excluded from the fit since they reflect localized deformations. The resulting expression for $\{\Delta_o\}$ is

$$\{\Delta_o\} = ([\alpha]^T [\alpha])^{-1} [\alpha]^T \{u\} \quad (6)$$

where

$$\{u\} = (\{u_1\}^T \ \{u_2\}^T \ \dots \ \{u_N\}^T)^T \quad (7)$$

$$[\alpha]^T = [[\alpha_1]^T \ [\alpha_2]^T \ \dots \ [\alpha_N]^T] \quad (8)$$

and

$$[\alpha_i] = \begin{bmatrix} 1 & 0 & 0 & 0 & z_i/l & -y_i/l \\ 0 & 1 & 0 & -z_i/l & 0 & x_i/l \\ 0 & 0 & 1 & y_i/l & -x_i/l & 0 \end{bmatrix} \quad (9)$$

in which $(x_i \ y_i \ z_i)$ are the coordinates of the i^{th} station with respect to the top center of the block. The vector $\{\Delta_o\}$ was calculated in the time domain, and then the amplitudes and phases of the components $\Delta_x, \Delta_y, \dots, l\theta_z$ were calculated for each test.

The scaled amplitude and the relative phase of the average EW, rocking and vertical rigid-body motion of the reaction block for EW excitation with one (Test 1) and two (Test 2) shakers are presented in Fig. 9. The recorded accelerations during Test 2 were transformed to scaled displacements by multiplication by the factor $(6.8/0.216) * (2\pi * 10/\omega)^2 / \omega^2$.

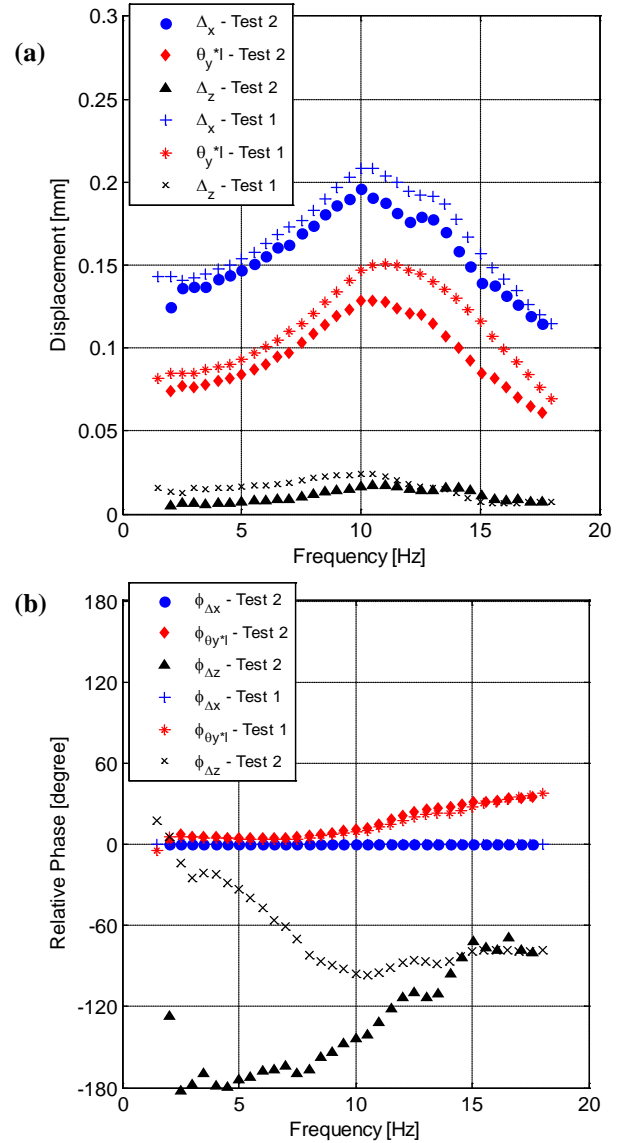


Fig. 9. (a) Amplitude and (b) relative phase of the average EW, rocking and vertical rigid-body motion of the reaction block for EW excitation (Tests 1 and 2).

The corresponding scaling factor for Test 1 was twice as large. The linearly scaled amplitudes correspond to a harmonic force

with constant amplitude of 6.8 MN. The most significant components of the average rigid-body motion are the EW translation and the rocking about the NS axis. The EW rigid body motion at the point of reference at the top center of the block is consistent with the averages T1 and T2 of the motion of the top of the block shown in Fig. 8a. The obtained average rocking motion is consistent with the vertical motion in the central area of the block (VT2 in Fig. 8b at a distance of 10.2m from the NS axis). There is also a small vertical motion of the center of the block due to asymmetry with respect to the NS axis associated with the empty soil pit and with lateral variations of soil properties. The transverse, torsional and rocking components about the EW axis are very small and are not shown in Fig. 9.

The results in Fig. 9a show that the scaled amplitudes for the response during Test1 (with one shaker) are proportionally slightly larger than the response during Test 2 (with two shakers). The explanation for this additional flexibility is that in Test 1 the shaker was located at the East end of the reaction block adjacent to then empty soil pit. In Test 2, the additional West shaker is adjacent to well-compacted backfill.

The pulsars on the shakers that were used to determine the phase of the harmonic force did not work properly during the tests. Consequently, the phase of the various response components with respect to the shaker force could not be obtained. Fig. 9b shows the relative phase of the rocking and vertical response with respect to the average EW displacement. The rocking response is essentially in phase with the EW displacement, while the average vertical displacement is 90- 150 degrees out of phase with respect to the EW displacement at 10 Hz.

COMPARISON OF SHAKER AND ACTUATOR INDUCED VIBRATIONS

During the initial characterization phase of the NEES/UCSD shake table, the platen was forced to undergo harmonic motions with frequencies of 4, 6, 8, 10, 12, 14, and 16 Hz (Tests SE9-16). The resulting EW motion of the reaction block was recorded at four stations at the top of the block and at two stations at the base (Fig. 10). The vertical motion of the top of the block was also recorded at the West and East ends of the block. The amplitudes of the total actuator force for tests SE9, SE10, SE11, SE12, SE14, SE15, and SE16 corresponded to 6.38, 6.48, 6.72, 6.67, 5.68, 6.58, and 6.88 MN, respectively. The actuator forces were calculated from the recorded accelerations of the platen and the effective mass of the platen (144,000 kg).

A sample of the accelerations recorded during Test SE12 with a frequency of 10 Hz is shown in Fig. 11. The amplitude of the force acting on the block during this test was 6.67 MN or 98% of the maximum nominal force that the actuators can exert. The results show that the longitudinal acceleration of the base and the central area at the top of the block reached about 10%

g, while the accelerations at the West and East walls reached values of 20 and 30% g, respectively. The vertical accelerations at the end walls were 180 degrees out of phase and had peak values of 10% g (West) and 25% g (East).

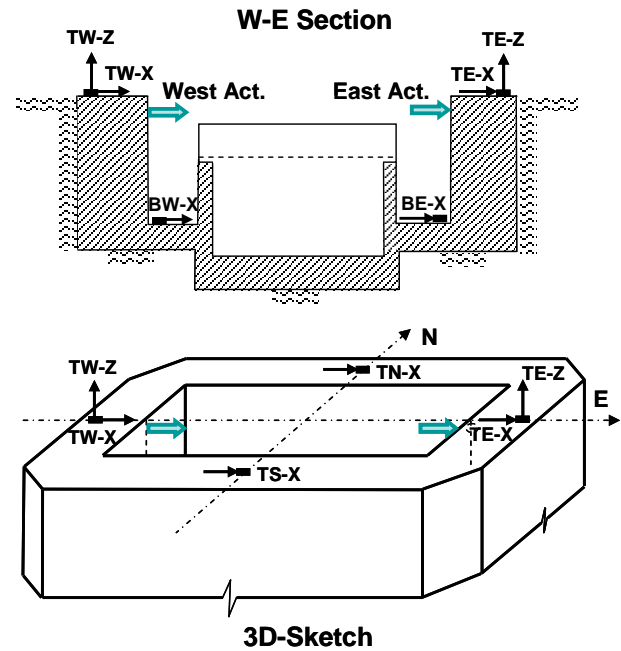


Fig. 10. Location of accelerometers during harmonic actuator tests SE9-SE16.

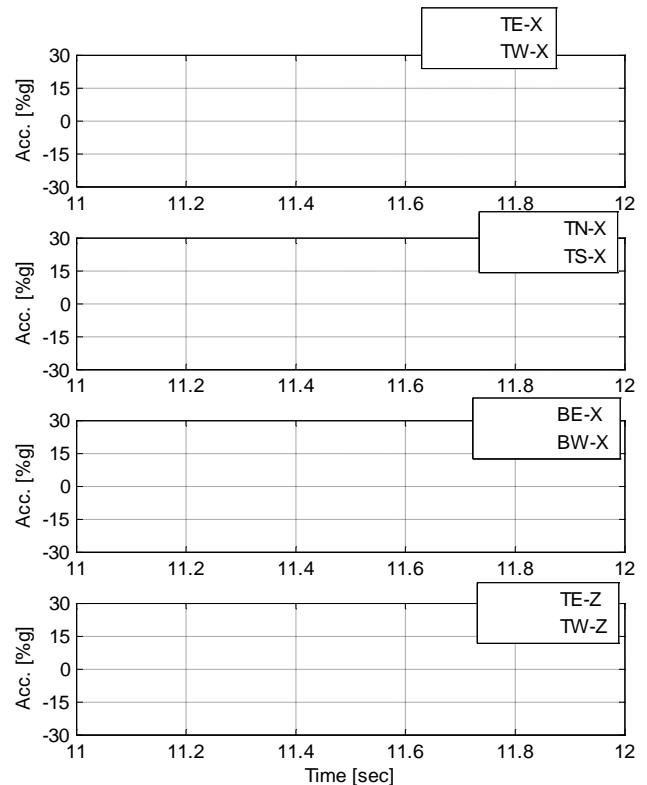


Fig. 11. Sample of acceleration time-histories recorded during harmonic actuator Test SE12 with a frequency of 10 Hz.

A comparison of the actuator and shaker-induced average rigid-body response of the reaction block during harmonic tests is presented in Fig. 12.

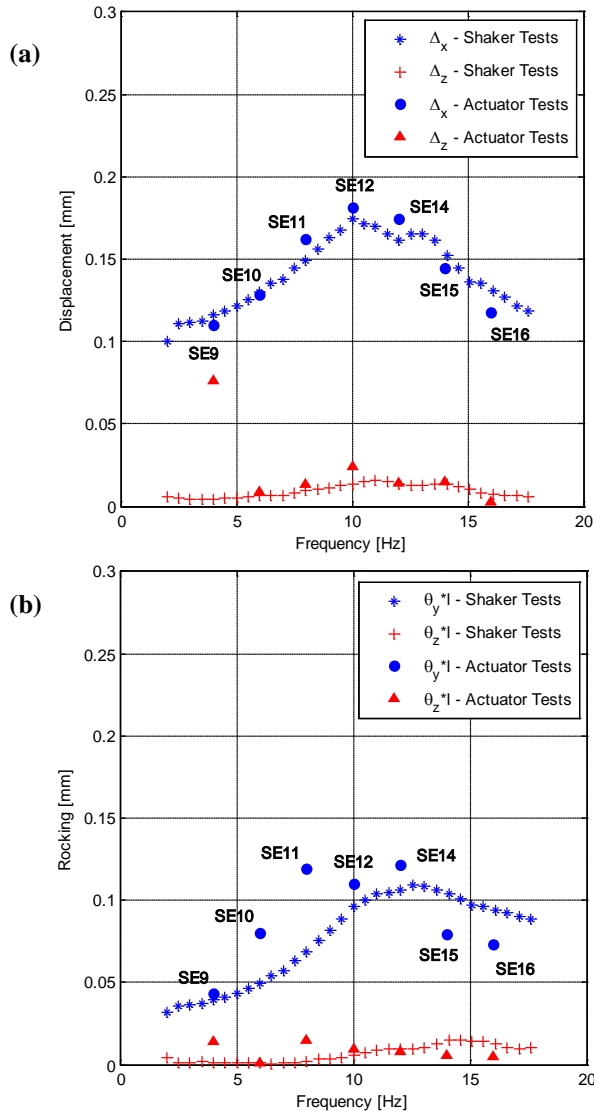


Fig. 12. Comparison of the actuator and shaker-induced response of the reaction block during harmonic tests. (a) Amplitudes of the scaled average rigid-body EW and vertical translation at the top of the block, and (b) Amplitudes of scaled average rigid-body rocking and torsion of the block.

The eccentric shaker results correspond to Test 2 with a total force of 0.216 MN at 10 Hz. The amplitudes have been linearly scaled to a force of 6.8 MN, and the rotation angles have been multiplied by the half-length of the reaction block $L=16.56$ m. The results in Fig. 12a correspond to the scaled amplitudes of the average rigid-body EW and vertical translations at the top of the block. Fig.12b shows the average rigid-body rocking of the block about the NS axis, and the torsion about the vertical axis. The components TE-x and TW-x recorded during actuator tests, and those recorded at stations RT4, RT5, RT9, RT10 during the shaker tests, are affected by

the local deformation of the end walls of the block, and were not included in the calculation of the average rigid-body-motions. The relatively good agreement between the two sets of normalized results is encouraging considering that, depending on frequency, the force level during the actuator tests was 13 to 185 times larger than that during the shaker tests ($6.67 \text{ MN}/0.216 \text{ MN}= 31$ times larger at 10 Hz). In addition, the moments exerted by the two types of forces were not comparable. The shakers exerted a force acting at an elevation higher than the location of the actuators. The results in Fig. 12 confirm that shaker-induced vibrations are a useful tool to study the dynamic response of foundations.

MOTION OF SURROUNDING SOIL

The patterns of deformation of the soil in the vicinity of the reaction block for EW excitation of the block is illustrated in Figs. 13 and 14. Figures 13a and b show the attenuation of the scaled EW (a) and vertical (b) displacements along the EW array of free-field ground stations for EW excitation of the reaction block at 10 Hz (Tests 14 and 17).

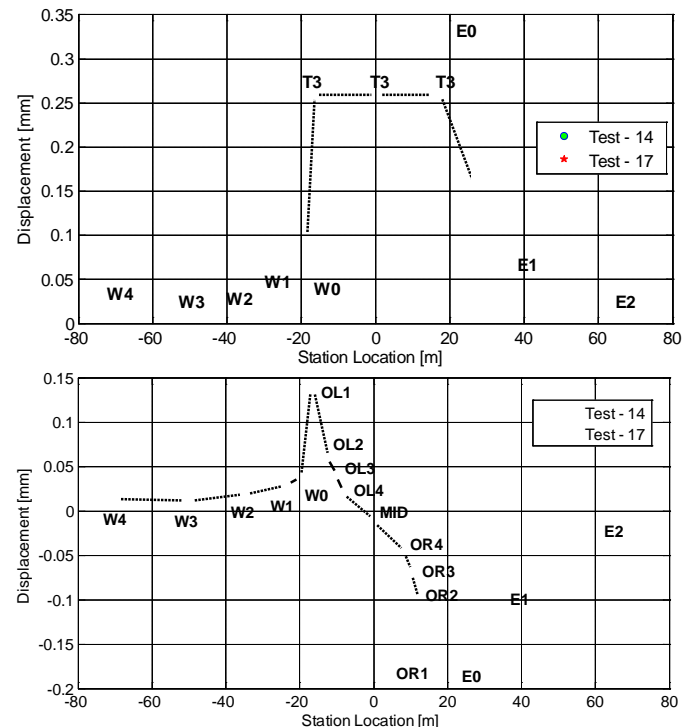


Fig. 13. Attenuation of the (a) EW and (b) Vertical scaled ground motions along the EW array of free-field ground stations for EW excitation of the reaction block at 10 Hz (Tests 14 and 17).

The corresponding attenuation of the scaled EW displacements along the NS array of free-field stations is shown in Fig. 14.

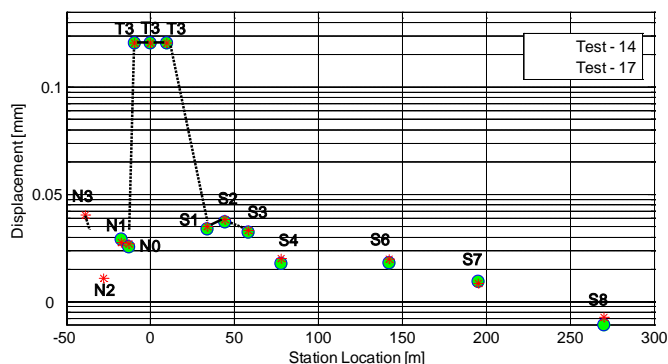


Fig. 14. Attenuation of the EW scaled ground motions along the NS array of free-field ground stations for EW excitation of the reaction block at 10 Hz (Tests 14 and 17).

The displacements of Test 14 with a total force of 0.216 MN (4 bricks per basket) at 10 Hz and Test 17 with a total force of 0.139 MN (1 brick per basket) also at 10 Hz have been linearly scaled to a force of 6.8 MN. A first observation is that the scaled results for Tests 14 and 17 are in excellent agreement indicating that the system is behaving linearly at this force level. A second observation is that the attenuation of the motion towards the East appears to be less than that to the West. This is probably a result of the fact that stations E0, E1 and E2 to the East were located inside the (then) empty soil pit while the stations to the West were on the undisturbed soil surface. Also, the attenuation towards the North appears to be faster than to the South.

CONCLUSIONS

It has been shown again that shaker-induced vibrations are a useful tool to study the dynamic interaction between foundations and the soil. In particular, properly scaled shaker-induced vibrations resulted in accurate estimates of the dynamic response of the reaction block of the NEES/UCSD shake table during actuator-induced vibrations. Good agreement was found between the two sets of scaled results even though the force levels during the actuator tests were, depending on frequency, 13 to 185 times larger than the level during the shaker tests ($6.67 \text{ MN}/0.216 \text{ MN} = 31$ times larger at 10 Hz). Also, the points of application of the shaker and actuator forces differed in elevation and, consequently, the moments exerted by the two types of forces were not fully comparable.

It has been shown experimentally that the displacements of the reaction block are sufficiently small not to interfere with the control of the shake table. For a harmonic force of 6.8 MN corresponding to the maximum force that the actuators can exert on the reaction block, the average rigid-body translation at the top of the block has amplitude of less than 0.2 mm. The corresponding amplitude of the average displacement at the ends of the West and East walls is 0.26 mm and the displacements at the centers of the West and East walls near the supports of the actuators are 0.42 and 0.64 mm,

respectively. These displacements are a very small fraction of the maximum stroke of the actuators which is 0.75 m. The controller of the shake table uses the absolute acceleration of the platen and the relative displacement between the platen and the reaction block as feedback to control the motion of the table. The implicit assumption, now validated, is that the relative displacement of the platen is similar to the absolute displacement.

The results obtained validate the unconventional design of the NEES/UCSD foundation block which took advantage of the natural conditions at the site in terms of high soil stiffness to build a lighter and considerably less costly foundation which resulted in a high characteristic frequency and a large effective damping ratio as opposed to the conventional design which relies on the use of massive foundations to achieve a low characteristic frequency. In the longitudinal EW direction, the frequency response curves for a harmonic force of constant amplitude show a broad peak at 10 Hz. Depending on the component considered, the dynamic amplification varies from 1.3 (motion on East and West walls at top of the block) to 1.67 (average rigid-body motion) suggesting an effective damping ratio between 32 and 42%, and a characteristic soil-foundation frequency between 11.2 and 12.5 Hz. These values are somewhat lower than those considered in the initial design for two main reasons: (i) the soil pit immediately adjacent to the reaction block was empty at the time of the tests, and (ii) cost cutting measures resulted in the trimming of the corners of the reaction block (compare Figs. 1 and 2). In addition, there are indications of a deeper and stiffer layer of soil at a depth of about 15 m which reduces the radiation damping into the soil.

The average rigid-body motion and the deformation patterns of the reaction block for longitudinal (EW) excitation of the block have been determined. The deformation patterns show out-of-plane deformation of all four walls and of the base slabs. The deformations are more pronounced on the East and West ends of the block and particularly on the East wall adjacent to the (then) empty soil pit. The coupled translation-rocking rigid-body motion of the block for longitudinal excitation has a peak at 10 Hz and shows a significant rocking component. All foundation-soil modes have small dynamic amplification showing a significant amount of radiation damping.

It is hoped that the data presented here will prove helpful in the validation of dynamic, three-dimensional, soil-foundation interaction analysis methods and associated computer codes. Data on the dynamic interaction through the soil between the adjacent foundations of the reaction block, control building and blast simulation facility, and additional data on the variation of the motion on the soil surface away from the reaction block will be presented elsewhere.

ACKNOWLEDGEMENTS

Support of this research by the National Science Foundation under Award No. CMMI-0301785 is gratefully acknowledged. Any opinions, findings, conclusions, or recommendations expressed in this publication are those of the authors and do not necessarily reflect the views of the sponsors. Some of the equipments used in the field program were provided by the PASSCAL facility of the Incorporated Research Institutions for Seismology (IRIS) through the PASSCAL Instrument Center at New Mexico Tech. The facilities of the IRIS Consortium are supported by the National Science Foundation under Cooperative Agreement EAR-0552316 and by the Department of Energy National Nuclear Security Administration.

The technical contributions made by D. Whang, S. Kang and R. S. Keowen of NEES/UCLA; R. Reyes, and E. Rocha of CICESE, Mexico; G. Acero, and B. Moaveni of UCSD; and L. Berman of NEES/UCSD during the experimental phase of this large-scale study are gratefully acknowledged. F. Vernon of the Scripps Institute of Oceanography at UCSD generously translated the extensive Antelope data files into more convenient Matlab files. G. Acero contributed the FE model of the reaction block shown in Fig. 2.

REFERENCES

Conte, J.P., J.E. Luco, J.I. Restrepo, F. Seible and L. Van Den Eide [2004], "UCSD-NEES Large High Performance Outdoor Shake Table", *Proc. 17-th ASCE Engineering Mechanics Conference*, University of Delaware, Newark, DE, June 13-16.

Geocon Inc. [2002], "Geotechnical Investigation, Structure Testing Facility, Elliot Field Station, University of California, San Diego, California", Report, April 19.

Ozcelik, O., J.P. Conte and J.E. Luco [2006], "Virtual Model of the UCSD-NEES High Performance Outdoor Shake Table", *Proc. Fourth World Conf. on Structural Control and Monitoring*, San Diego, California, July 11-13, Paper No. 285.

Ozcelik, O., J.E. Luco, J.P. Conte, T.L. Trombetti and J.I. Restrepo [2008a], "Experimental Characterization, Modeling and Identification of the NEES-UCSD Shake Table Mechanical System", *Earthquake Engineering and Structural Dynamics*, 37, pp. 243-26.

Ozcelik, O., J.E. Luco and J.P. Conte [2008b], "Identification of the Mechanical Subsystem of the NEES-UCSD Shake Table by a Least-Squares Approach", *Journal of Engineering Mechanics*, ASCE, 134(1), pp. 23-34.

Stewart, J.P., D.H. Whang, J.W. Wallace and R.L. Nigbor, [2005], "Field testing capabilities of the NEES@UCLA equipment site for soil-structure interaction applications", in *Earthquake Engineering and Soil Dynamics, Proc. of Sessions of the Geo-Frontiers 2005 Congress*, ASCE Geotech. Special Publication 133, (R.W. Boulanger, M. Deewolder, N. Gucunski, C. H. Juang, M. E. Kalinsky, S. L. Kramer, M. Manzari and J. Pauschke, eds.), 9 pages (electronic file).

Van Den Eide, L., J.I. Restrepo, J.P. Conte, J.E. Luco, F. Seible, A. Filiatrault, A. Clark, A. Johnson, M. Gram, D. Kusner and B. Thoen [2004], "Development of the George E. Brown, Jr. Network for Earthquake Engineering Simulation (NEES) Large High Performance Outdoor Shake Table at the University of California, San Diego", *Proc. 13th World Conf. on Earthquake Engineering*, Vancouver, B.C., Canada, August 1-6, Paper No. 3281.